Int. J. Electrochem. Sci., 8 **(2013)** 1794 - 1801

International Journal of
ELECTROCHEMICAL
SCIENCE
www.electrochemsci.org

Synthesis of In_2O_3 Nanocrystals via Hydro/Solvothermal Route and Their Photoluminescence Properties

Zhuangdong Yuan, Jing Zhang, Guodong Liu[*]

Department of Chemistry and Chemical Engineering, Key laboratory for Inorganic Chemistry, Institute of Functional Materials, Jining University, Jining 273155 P. R. China
[*]E-mail: liugd001@hotmail.com

Received: 5 September 2012 / *Accepted:* 5 January 2013 / *Published:* 1 February 2013

In the hydro/solvothermal system, morphologies and phases of the products can be controlled through adjusting the hydrolysis reaction of indium salt. In ethanol solvothermal reaction system, In_2O_3 nanoparticles were produced directly, which can be proposed as a "dissolution-recrystallization" mechanism, and the driving force is the lower solubility of the In_2O_3 compared to the $In(OH)_3$ in the system. In the hydrothermal system, $In(OH)_3$ nanobelts were obtained. After heat-treatment at 300 °C, In_2O_3 single crystals nanobelts were produced, which can keep the morphologies and sizes of precursors. The room temperature PL spectra of as-prepared In_2O_3 nanoparticles and nanobelts are clearly different, which is due to existence of different oxide-deficiency states from the different synthesis routes.

Keywords: In_2O_3 Nanocrystals; Solution-phase Synthesis; Photoluminescence

1. INTRODUCTION

Indium oxide (In_2O_3), an important *n*-type III-VI semiconductor, has attracted considerable attention because of the peculiar electronic and optical properties and increasingly extensive applications in solar cells [1], sensors [2], electrocatalyst [3,4] and nanoscale transistors [5,6] etc. In the past decade, many efforts have been made concerning the preparation of In_2O_3 nanostructures with different morphologies [7] have been successfully prepared, and various methods such as chemical vapor deposition, [8] hot-injection technique, [9] organic solution synthesis, [10] hydro/solvothermal route, [11] sol-gel technique [12] and etc have been developed. Among so many solution synthesis routes above, the calcination of corresponding hydrolysis precursors, such as $In(OH)_3$ and InOOH is necessary, which can be concluded that H_2O plays a crucial role and hydrolyzation of In^{3+} is absolutely necessary.

So far, the influences of reactional precursors, temperature, time, surfactants on morphologies, sizes, and phases of products have been deeply researched. However, the influence of H_2O in solution system is rarely reported. As a polar solvent, H_2O plays sevaral roles in hydro/solvorhermal process, which can be summarized: (i) As solvent: Reaction substances dissolved and temperature and pressure transferred medium. (ii)As reaction substance: take part in the hydrolysis reaction to form oxide or hydroxide. (iii) (3) Influence the number of hydroxyl on the surface of obtained nanocrystals, and further affect the ir aggregation. Hence, How to use the adjustment of systemic H_2O to control solution-phase synthesis nanomaterials has an important research value. Herein, a simple hydro/solvothermal route to the In_2O_3 nanocrystals with different morphologies by using $In(NO_3)_3$ as indium source was introduced. Through adjusting the systemic amount of water, the In^{3+} hydrolysis reaction can be controlled. Of course, the phases and morphologies of products also can be controlled.

2. EXPERIMENTS

2.1. Synthesis

In a typical synthesis, 0.046 g (0.125 mmol) of $In(NO_3)_3 \cdot 4H_2O$ and 0.114 g (0.375 mmol) sodium oleate were added into a 15 mL Teflon-lined autoclave respectively. After putting mixed solvent of H_2O and ethanol 10 mL into the autoclave, the autoclave was sealed and put into an oven at 200 °C for 3 h. Then, the autoclave was allowed to cool to room temperature naturally. The product was collected by centrifugization, washed with ethanol for several times and dried at 60 °C for 2 h in air.

2.2. Transformation into In_2O_3

The as-prepared $In(OH)_3$ nanocrystals were calcined in a boat crucible at a temperature of 300 ^oC and maintained for 2 h in air.

2.3. Characterization. Characterization

X-ray diffraction (XRD) patterns of the samples were recorded on an X-ray diffractometer (Rigaku D/Max 2200PC) with a graphite monochromator and CuKα radiation (λ=0.15148 nm) in the range of 10-80° at room temperature while the voltage and electric current were held at 40 kV and 20 mA. The morphology and microstructure of the products were determined by transmission electron microscopy (TEM, JEM-100CXII) with an accelerating voltage of 80 kV and high-resolution TEM (HR-TEM, GEOL-2010) with an accelerating voltage of 200 kV. The PL spectrum of In_2O_3 nanostructures was measured on a Hitachi M-850 fluorescence spectrophotometer at room temperature with the excitation wavelength of 243 nm. UV-vis absorption spectra technique (UVvis spectrometer, Lambda-35, Perkin-Elmer) was used to characterize the absorbance of the products.

3. RESULTS AND DISCUSSION

Table1. Phases and Morphologies of Products obtained from different system

Volume of Mixed Solvent	H_2O (mL)	Product	Morphology
10 mL	0 mL	S1: C-In_2O_3	Nanoparticles
	0.5 mL	S2: Mixture of InOOH, $In(OH)_3$ and C-In_2O_3	Nanoparticles
	1.5 mL	S3: $In(OH)_3$, InOOH	Nanoparticles and nanorods
	5.0 mL	$In(OH)_3$	Nanoparticles, nanorods and nanobelts
	10.0 mL	S4: $In(OH)_3$	Nanobelts

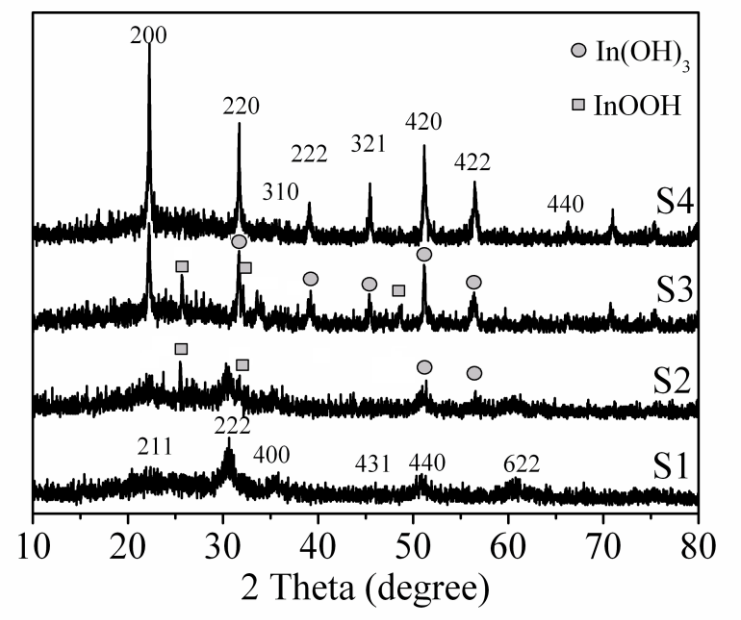

Figure 1. XRD patterns of Products obtained from different system. Amount of H_2O in the system S1 (0 mL), S2 (0.5 mL), S3 (1.5 mL), S4 (10 mL)

Through adjusting the systemic amount of water, different kinds of products were obtained. (See Table 1 and Figure 1) The XRD pattern of the sample obtained in ethanol solvothermal route, which is denoted as S1, can be indexed to the cubic In_2O_3 (JCPDS, No. 65-3170), no other peaks can be observed, revealing its phase-pure cubic structures. The size of S1 is 5.5 nm calculated from the Scherrer equation. Further calculation revealed that the cell parameters of the sample is 1.0142 nm, which is in well agreement with the reported data of a=1.0140 nm (JCPDS, No. 65-3170). The data was collected using KCl as standard graph and the scan speed was one degree per minute. TEM images (Figure 2) of S1 indicate that the In_2O_3 nanocrystals show as regular nanoparticles with the size ca.6 nm. (Figure 2a) The HR-TEM image shows clear continuous lattice fringes in one nanocrystal,

indicating its single crystalline nature and high crystallinity. The interplanar distances of 0.293 nm can be readily indexed to {222} planes of cubic In_2O_3. (Figure 2b) As known, the metal alkoxide easily hydrolyzes to form metal hydroxide or oxide. In ethanol solvothermal reaction system, hydrolysis reaction between In^{3+} and H_2O were occurred to form indium hydroxide. (Figure 3b) The generated $In(OH)_3$ from hydrolysis of indium salt further dehydrated to form In_2O_3 nancrystals which can be proposed as a "dissolution-recrystallization" mechanism, and the driving force is the lower solubility of the In_2O_3 compared to the $In(OH)_3$ in the system.

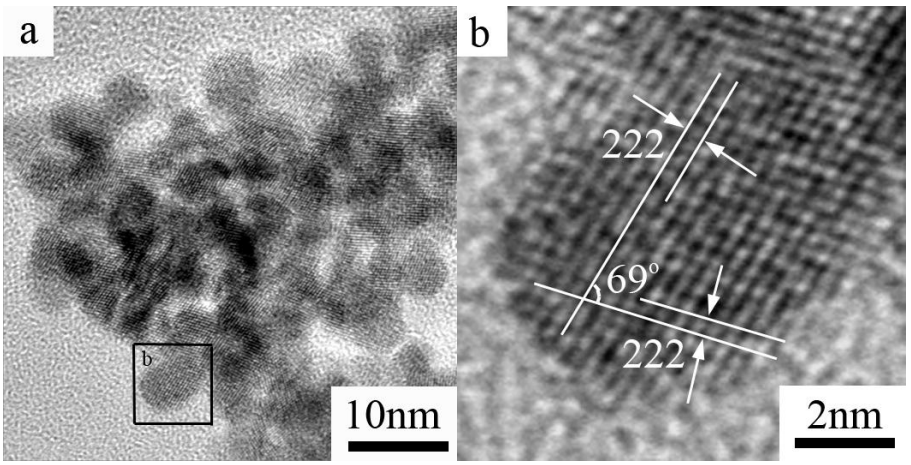

Figure 2. TEM image (a) and HR-TEM of S1

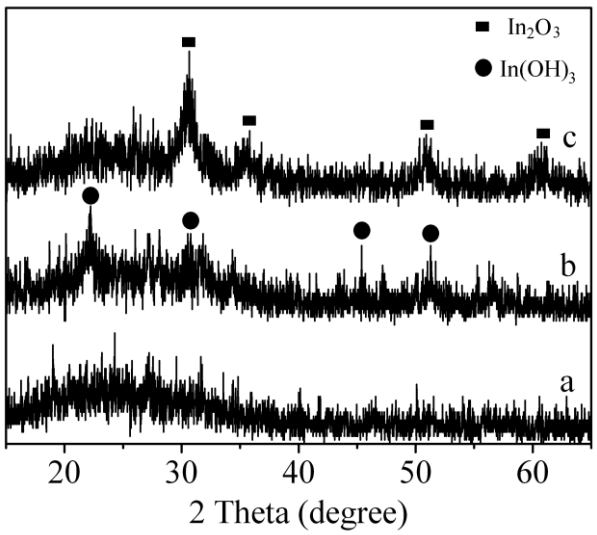

Figure 3. XRD patterns of Products obtained from different time during ethanol solvothermal procedure. (a)0.5 h, (b)1.0 h, (c) 3.0 h.

The XRD pattern of the sample obtained in hydrothermal route, which is denoted as S4, can be indexed to the $In(OH)_3$ (JCPDS, No. 76-1464), no other peaks can be observed, revealing its phase-pure cubic structures. (See Figure 1 and Figure 4a) TEM images (Figure 5a,b) of S4 indicate that

$In(OH)_3$ nanocrystals show as regular nanobelts with the width ca.20 nm and more than 300 nm long. These nanobelts were partially decomposed under electron beam irradiation. (Indicated by an arrow in Figure 5b) In some undecomposed $In(OH)_3$ area, the interplane distance of lattice fringes is about 0.29 nm, which corresponds to that of the (220) face of $In(OH)_3$ and indicates these rods grow along the [100] direction. In the hydrothermal system, the indium ions completely hydrolyzed. Due to the alkali of sodium oleate in water can provide plenty of OH^- to promote the growth of nanocrystals, the $In(OH)_3$ belt-like structure obtained. Furthermore, $In(OH)_3$ is an ionic compound, and the surface-electron and dipole-dipole interactions are important factors to the nanocrystal growth. In a higher polar solvent, such as H_2O, the dipole moments are larger, so they have stronger dipole-dipole interactions between nanocrystals. The dipole-dipole interactions may cause the nanocrystals to favor growth in a particular direction. An increase in solvent polarity will lead nanocrystals to grow faster along a particular direction, resulting in beltlike nanocrystals. [13]

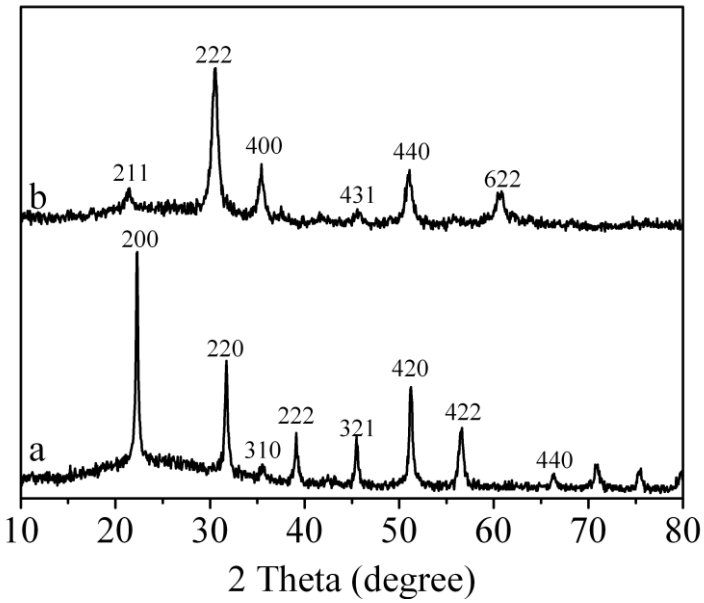

Figure 4. XRD patterns of Product S4 (a) and its calcined product In_2O_3 (b)

Like other metal hydroxides, indium hydroxide can dehydrate to form indium oxides upon heating. To keep the original morphologies from $In(OH)_3$ possible, the heating temperatures were selected at a little above of the phase-changing temperature ,300 °C for $In(OH)_3$. After heat-treatment at 300 °C, In_2O_3 single crystals nanobelts were produced. Figure 4b shows the XRD patterns of as-prepared In_2O_3 nanocrystals, which indicate that all of these samples are purely cubic In_2O_3. They are all in good agreement with the reports in the literature (cubic In_2O_3, JCPDS, No. 65-3170). The TEM images (Figure 5c,d) indicate that all of these samples can keep the morphologies and sizes to a certain extent after annealing. Products obtained from systems which amount of H_2O are between 0.5 to 5 mL are mixtures of In_2O_3, InOOH and $In(OH)_3$. (See Figure 1) Their morphologies are also in muddle. (See Figure 6a-c)

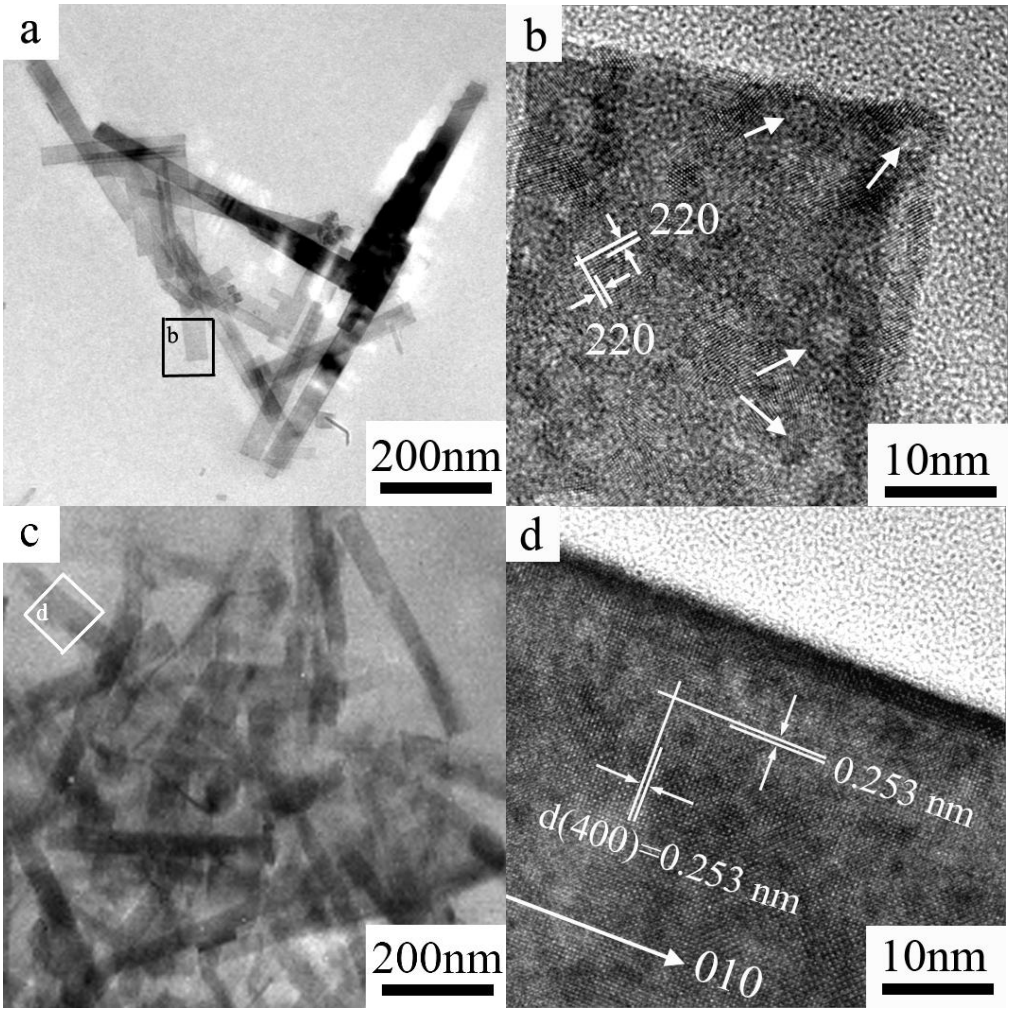

Figure 5. TEM images (a, b) of S4 and its calcined product In_2O_3 (c, d)

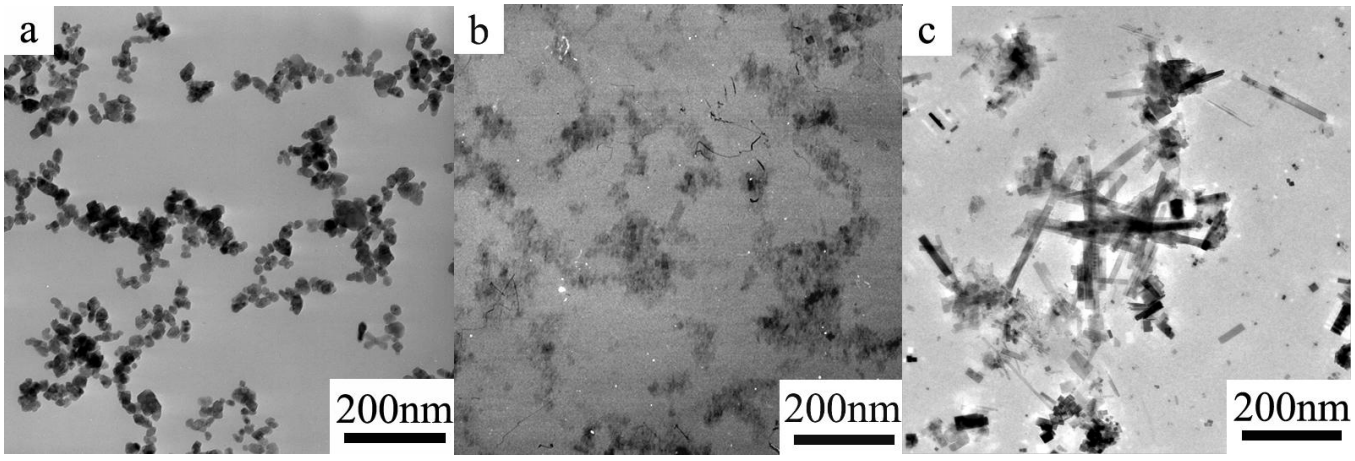

Figure 6. TEM images of products obtained from different system. Amount of H_2O (a) 0.5 mL, (b) 1.5 mL, (c) 5 mL.

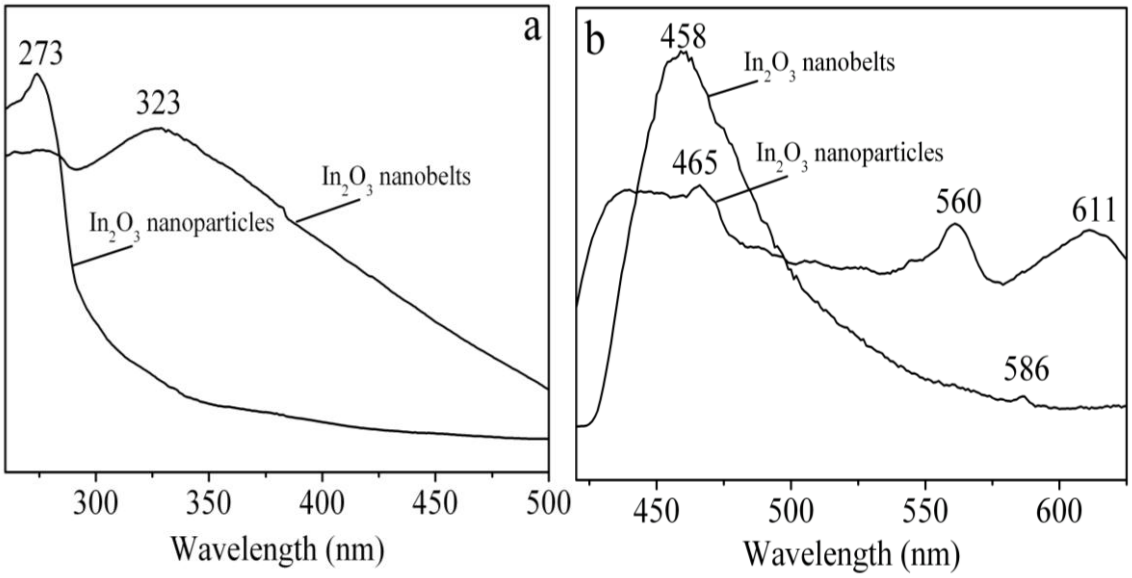

Figure 7. UV-vis spectra (a) and PL spectra (b) of In_2O_3 nanocrystals.

The Uv-vis absorption spectra of In_2O_3 nanocrystals with different morphologies show absorption maxima at 273 nm and 323 nm (Figure 7a).Compared to the absorption at 330 nm (3.75 eV) of bulk In_2O_3 [14], a blue-shift is observed due to the weak quantum confinement effect [15]. The PL emissions of the In_2O_3 nanocrystals with different morphologies are obviously different. (Figure 7b, all the samples excited at 243 nm, room temperature) PL peaks of In_2O_3 nanoparticles obtained from solvothermal route were centered at 465 nm (blue), 560 nm, and 611 nm (orange). However, PL peaks of In_2O_3 nanobelts mainly focused at 458 nm (blue). Cubic In_2O_3, as a typical n-type semiconductor, has an oxygen-deficient fluorite structure with twice the unit-cell edge of the corresponding fluorite cell and with 1/4 of the anions missing in an ordered way, which would induce the formation of new energy levels in the band gap [16]. The room temperature PL spectra of as-prepared In_2O_3 nanoparticles and nanobelts are clearly different, which is due to existence of different oxide-deficiency states from the different synthesis routes.

4. CONCLUSION

In summary, in the hydro/solvothermal system, $In(NO_3)_3 \bullet 4H_2O$ was used as the indium source, adjusting the hydrolysis reaction of indium salt in order to control morphologies of the products. In ethanol solvothermal reaction system, the generated $In(OH)_3$ from hydrolysis of indium salt further dehydrated to form In_2O_3 nancrystals which can be proposed as a “dissolution-recrystallization” mechanism, and the driving force is the lower solubility of the In_2O_3 compared to the $In(OH)_3$ in the system. In the hydrothermal system, the indium ions completely hydrolyzed. Due to the alkali of sodium oleate in water can provide plenty of OH^- to promote the growth of nanocrystals, the $In(OH)_3$ belt-like structure obtained. After heat-treatment at 300 °C, In_2O_3 single crystals nanobelts were produced. The room temperature PL spectra of as-prepared In_2O_3 nanoparticles and nanobelts are

clearly different, which is due to existence of different oxide-deficiency states from the different synthesis routes.

ACKNOWLEDGEMENTS.
This work is supported by Doctoral Foundation of Shandong Province (BS2010CL009) and Pre-research Fund of National Foundation (2011YYJJ01).

References

1. T. H. Tsai, S. C. Chiou, S. M. Chen, *Int. J. Electrochem. Sci.*, 6 (2011) 3333-3343.
2. T. M.Justin, Y. Y.Jackie, *Chem. Mater.* 19, (2007) 1009-1015.
3. R. S. Henrique1, R. F. B. De Souza, J. C. M. Silva, J. M. S. Ayoub, R. M. Piasentin, M. Linardi, E. V. Spinacé1, M. C. Santos, A.O.Neto, *Int. J. Electrochem. Sci.*, 7 (2012) 2036-2046.
4. J. Parrondo1, R. Santhanam1, F. Mijangos, B. Rambabu, *Int. J. Electrochem. Sci.*, 5 (2010) 1342 - 1354
5. J. Liu, Y. Zhu, J. Liang, Y. Qian, *Int. J. Electrochem. Sci.*, 7 (2012) 5574-5580.
6. B. Devadas, M. Rajkumar, S. M. Chen, R.. Saraswathi, *Int. J. Electrochem. Sci.*, 7 (2012) 333-3349.
7. G. Liu, *Int. J. Electrochem. Sci.*, 6 (2011) 2162-2170.
8. C.Liang, G.Meng, Y.Lei, F. Phillipp, L. Zhang, *Adv. Mater.* 13 (2001)1330-1333.
9. J.Lao, J.Huang, D.Wang, Z.Ren, *Adv. Mater.* 16 (2004) 65-69.
10. C.Chen, D.Chen, X.Jiao, C.Wang, *Chem. Commun.* (2006) 4632-4624.
11. P. F. Yu, W. Q. Jie, T. Wang, *J. Mater. Sci.*, 46, 3189-3191 (2011)
12. J. W.Elam, A. B. F.Martinson, M. J.Pellin, J. T. Hupp, *Chem. Mater.* 18 (2006) 3571-3578.
13. Z. Zhuang, Q. Peng, J. Liu, X. Wang, Y. Li, *Inorg. Chem.* 46 (2007) 5179-5187.
14. Q. Liu, W. Lu, A. Ma, J. Tang, J. Lin, J. Y. Fang, *J. Am. Chem. Soc.* 127 (2005) 5276-5277.
15. C. Lee, M. Kim, T. Kim. A. Kim, J. Paek, J. Lee, Choi, S.; Kim, K.; Park, J.; Lee, K. *J. Am. Chem. Soc.* 128 (2006) 9326-9327.
16. H.Cao, X.Qiu, Y.Liang, Q. Zhu *Appl. Phys. Lett*. 83 (2003) 761-763.